SIRM 2013 – 10th International Conference on Vibrations in Rotating Machines,
Berlin, Germany, 25. – 27. February 2013

On electromechanical dynamic coupling effects in the semi-actively controlled rotating machine drive system driven by the induction motor

Tomasz Szolc [1], Maciej Michajłow [2], Robert Konowrocki [3]

Institute of Fundamental Technological Research of the Polish Academy of Sciences, ul. Pawińskiego 5 B, 02-106 Warsaw, Poland, [1] tszolc@ippt.gov.pl , [2] mmich@ippt.gov.pl, [3] rkonow@ippt.gov.pl

Abstract

In the paper there is studied dynamic electromechanical interaction between the geared drive system of a rotating machine and the driving induction (asynchronous) motor. The investigations are performed by the use of experimental measurements carried out on the real object as well as by means of a theoretical approach using a circuit model of the electric motor in the form of Park's equations and the advanced drive system hybrid, i.e. discrete-continuous, mechanical model of an identical structure and parameters as the classical preliminarily applied one-dimensional finite element model. The experimental and theoretical considerations are focused on the steady-state operating conditions, where severe torsional vibrations are excited by variable components of the driven machine retarding torque as well as by the electromagnetic torque generated by the induction motor. The qualitative analysis is performed by means of the harmonic balance method applied for Park's equations and using the modal approach for the experimentally identified mechanical model. In order to minimize torsional vibration amplitudes induced by the electromechanical interaction in the considered system, the semi-active control technique based on actuators with the magneto-rheological fluid has been tested.

1 Introduction

Torsional vibrations of machine drive systems driven by electric motors usually result in a motor rotor angular velocity fluctuation causing more or less severe perturbations of the generated electromagnetic torque. Thus, mechanical vibrations become coupled with electrical oscillations of electric currents in the motor windings. Commonly observed recently increasing power and technical demands made to rotating machinery driven by several types of electric motors motivate engineers and scientists to investigate better and better dynamic phenomena caused by electromechanical coupling effects between the mechanical and electrical parts of these objects. From numerous papers published during last years, e.g. [2,3,9], it follows that the electromechanical coupling in the form of dynamic interaction between torsional vibrations of the drive trains and additional fluctuation components of the electric currents in the electric motor stator and rotor windings is able to induce dangerous unexpected resonance oscillations. Moreover, the electromagnetic torque generated by the electric motor can more or less significantly change dynamic properties of the machine drive system, [5]. These detrimental phenomena are observed in steady-state operating conditions as well as during start-ups and run-downs, particularly in the case of devices equipped with electronically controlled motor converters in the form of so the called 'variable speed drives' (VSD), [2,9]. Thus, these problems began to be more and more intensively studied experimentally and theoretically using various mechanical models of drive systems and electrical models of the motors. At the beginning, because of natural computational difficulties, the mechanical and electrical interaction problems were solved separately by means of very simple discrete drive system models, see [4], and using circuit models of induction and synchronous motors, as e.g. in [1]. Nevertheless, owing to the permanent general rise of computer power, these so important problems were gradually studied as mutually coupled. In this field the most popular are simple multi-spring-mass discrete models of the drive trains and circuit models of the synchronous motors commonly applied e.g. in the complex torque coefficient method described in [6]. The spatial finite element model of the electromagnetic flux in the asynchronous and synchronous motors have been used in [3] in order to determine the electromagnetic rotor-to-stator rotational

stiffness and damping coefficient by means of the transmittances of motor torque fluctuation due to an 'a priori' imposed rotor angular velocity perturbations. These stiffness and damping coefficients are used next as parameters of the visco-elastic electromagnetic springs attached to simple discrete or structural finite element mechanical drive system models as an equivalent representation of the electromechanical coupling interaction.

The electromagnetic rotor-to-stator rotational stiffness and damping coefficients additionally expressed as functions of drive system dynamic parameters have been determined in [5] by means of the advanced structural hybrid model of the drive system coupled with the asynchronous motor circuit model. In that paper a severity of electromechanical coupling effects was studied for several drive systems of diverse dynamic properties driven by various asynchronous motors. In the presented paper this approach is going to be continued in order to investigate deeper sensitivity to resonances as well as to an unexpected severe amplification of torsional vibration amplitudes occurring at non-resonant excitation frequencies. In order to suppress torsional vibration amplitudes there is applied the semi-active control technique, described in details in [6], basing on the actuator in the form linear magneto-rheological dampers co-operating with the visco-elastically suspended planetary gear housing. By means of this control technique the abovementioned detrimental torsional fluctuations induced by the electromechanical coupling effects are going to be attenuated.

2 Fundamental assumptions and mathematical formulation of the problem

In order to investigate a character of the electromechanical coupling the possibly realistic and reliable mechanical model of the drive system as well as the electrical model of the driving motor are applied.

2.1 Modelling of the mechanical system

In this paper dynamic investigations of the entire drive system are performed by means of the one-dimensional hybrid structural model consisting of finite continuous visco-elastic macro-elements and rigid bodies. In this model by the torsionally deformable cylindrical macro-elements of continuously distributed inertial-visco-elastic properties there are substituted successive cylindrical segments of the stepped shafts and coupling disks, as presented in Figure 1. In order to obtain a sufficiently accurate representation of the real object the visco-elastic macro-elements in the hybrid model are characterized by the geometric cross-sectional polar moments of inertia J_{Ei} responsible for their elastic and inertial properties as well as by the separate layers of the polar moments of inertia J_{Ii} responsible for their inertial properties only, i=1,2,…,n, where n is the total number of macro-elements in the considered hybrid model. The inertias of gear-wheels and driven machine working tools are represented by rigid bodies attached to the appropriate macro-element cross-sections.

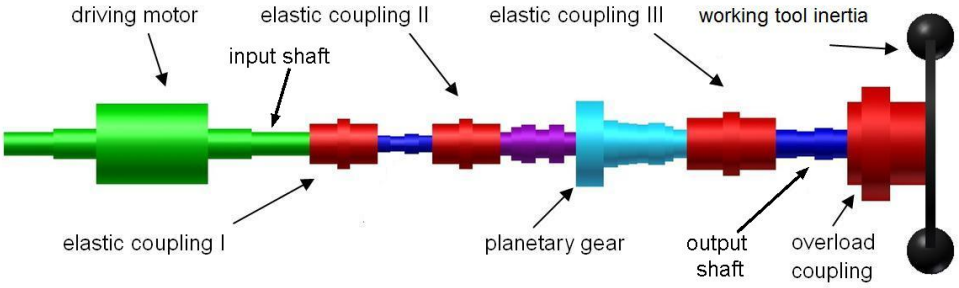

Figure 1: Hybrid mechanical model of the drive system (regarded as a 'free-free' system)

Torsional motion of cross-sections of each visco-elastic macro-element is governed by the hyperbolic partial differential equations of the wave type

$$G_i J_{Ei}\left(1+\tau\frac{\partial}{\partial t}\right)\frac{\partial^2\theta_i(x,t)}{\partial x^2}-c_i\frac{\partial\theta_i(x,t)}{\partial t}-\rho\left(J_{Ei}+J_{Ii}\right)\frac{\partial^2\theta_i(x,t)}{\partial t^2}=q_i(x,t), \tag{1}$$

where $\theta_i(x,t)$ is the angular displacement with respect to the shaft rotation with the average angular velocity Ω, τ denotes the retardation time in the Voigt model of material damping, G_i is the Kirchhoff modulus of the model i-th macro-element material and c_i denotes the coefficient of external (absolute) damping. The external active, passive and control torques are continuously distributed along the respective macro-elements of the lengths l_i. These torques are described by the two-argument function $q_i(x,t)$, where x is the spatial co-ordinate and t denotes time. Mutual connections of the successive macro-elements creating the stepped shaft as well as their interactions with the rigid bodies are described by equations of boundary conditions formulated for the macro-element extreme cross-sections. These equations enclose geometrical conditions of conformity for rotational

displacements as well as equilibrium conditions for external and internal visco-elastic torques. The mathematical description and solution for such hybrid models have been demonstrated in details e.g. in [7]. Solving the differential eigenvalue problem for the orthogonal linear system and an application of the Fourier solution in the form of series of developments in eigenfunctions lead to the set of modal ordinary differential equations:

$$\ddot{\xi}_m(t) + \left(\beta + \tau\omega_m^2\right)\dot{\xi}_m(t) + \omega_m^2\xi_m(t) = \frac{1}{\gamma_m^2}\left(X_m^S \cdot T_{el}(t) - X_m^R \cdot M_r(t)\right), \quad m = 1,2,\ldots \qquad (2)$$

where ω_m are the successive natural frequencies of the drive system, β denotes the coefficient of external damping assumed here as proportional one to the modal masses γ_m^2, $T_{el}(t)$ denotes the external torque generated by the electric motor, $M_r(t)$ is the driven machine retarding torque and X_m^S, X_m^R are the scaled by proper maxima modal displacements corresponding respectively to the electric motor and driven machine working tool locations in the hybrid model. A fast convergence of the applied Fourier solution enables us to reduce the number of the modal equations to solve in order to obtain a sufficient accuracy of results in the given range of frequency. Here, it is necessary to solve only 6÷10 modal equations (2), even in cases of very complex mechanical systems, contrary to the classical one-dimensional discretized beam finite element formulation leading usually to large numbers of motion equations corresponding each to more than one hundred or many hundreds degrees of freedom (if the artificial and often error-prone model reduction algorithms are not applied).

a) b)

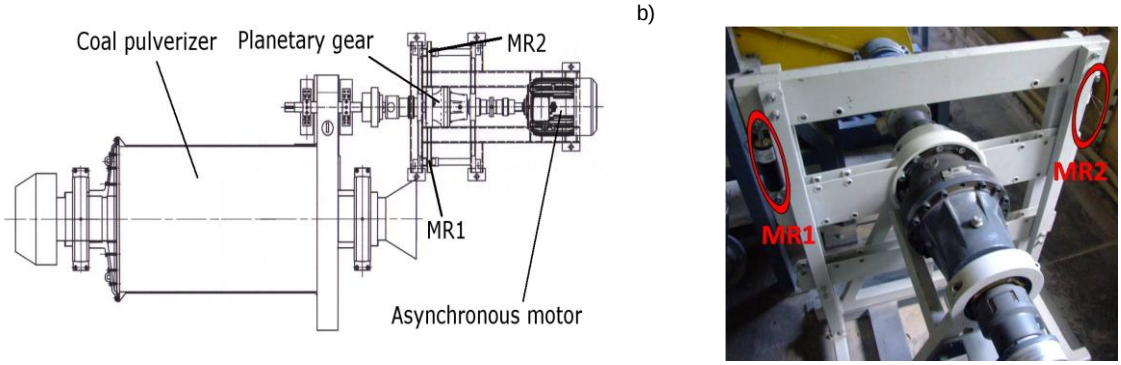

Figure2: Coal pulverizer drive system (a) and the actuator with two linear MRF dampers MR1 and MR2 (b).

In order to perform a semi-active torsional vibration control for the rotating machine drive system the actuator consisting of two or four linear magneto-rheological dampers controlling rotational motion of the visco-elastically suspended planetary gear housing can be applied similarly as in [6]. Such semi-active control technique has been successfully applied for the shown in Fig. 2a coal pulverizer geared drive system driven by the asynchronous motor using the mentioned above magneto-rheological actuator presented in Fig. 2b. By means of properly controlled damping properties of this visco-elastic suspension of the gear housing control forces generated by the linear dampers are imposed on the drive system in the form of control damping torques. According to the mathematical solution of the problem derived in [6] for the drive system model with this actuator, these damping torques can be regarded as a response-dependent control external excitation. Then, by a transformation of them into the space of modal coordinates $\xi_m(t)$ and upon a proper rearrangement of the modal independent equations (2), the following set of coupled modal equations is obtained:

$$\mathbf{M}_0\ddot{\mathbf{r}}(t) + \mathbf{D}(C_0(t,\dot{\mathbf{r}}(t))) \cdot \dot{\mathbf{r}}(t) + \mathbf{K}_0\mathbf{r}(t) = \mathbf{F}(t,\dot{\mathbf{r}}(t)), \qquad (3)$$

where $\mathbf{D}(C_0(t)) = \mathbf{D}_0 + \mathbf{D}_C(C_0(t,\dot{\mathbf{r}}(t)))$.

The symbols $\mathbf{M}_0$, $\mathbf{K}_0$ and $\mathbf{D}_0$ denote, respectively, the constant diagonal modal mass, stiffness and damping matrices. The full matrix $\mathbf{D}_C(C_0(t,\dot{\mathbf{r}}(t)))$ plays here a role of the semi-active control matrix and the symbol $\mathbf{F}(t,\dot{\mathbf{r}}(t))$ denotes the response dependent external excitation vector due to the electromagnetic torque generated by the electric motor and due to the retarding torque produced by the driven machine. The Lagrange coordinate vector $\mathbf{r}(t)$ consists of the unknown time functions $\xi_m(t)$ in the Fourier solutions, m=1,2,… . These equations are mutually coupled by the out-of-diagonal terms in matrix $\mathbf{D}$ regarded as external excitations developed in series in the base of orthogonal analytical eigenfunctions. Similarly as in the case of solving the mutually independent modal equations (2), the number of coupled equations (3) also corresponds to the number of the torsional eigenmodes taken into consideration in the range of frequency of interest. A fast convergence of the applied Fourier solution enables us to reduce the appropriate number of the modal equations to solve in order to obtain a sufficient accuracy of results in the given range of frequency.

2.2 Modeling of the electrical system

From the viewpoint of electromechanical coupling investigation, the properly advanced circuit model of the electric motor seems to be sufficiently accurate. In the case of the symmetrical three-phase asynchronous motor electric current oscillations in its windings are described by the six circuit voltage equations transformed next into the system of four Park's equations in the so called '$\alpha\beta$-dq' reference system

$$\begin{bmatrix} \sqrt{\frac{3}{2}}U\cos(2\pi f_0 t) \\ \sqrt{\frac{3}{2}}U\sin(2\pi f_0 t) \\ 0 \\ 0 \end{bmatrix} = \begin{bmatrix} L_1+\frac{1}{2}M & 0 & \frac{3}{2}M & 0 \\ 0 & L_1+\frac{1}{2}M & 0 & \frac{3}{2}M \\ \frac{3}{2}M & 0 & L_2'+\frac{1}{2}M & 0 \\ 0 & \frac{3}{2}M & 0 & L_2'+\frac{1}{2}M \end{bmatrix} \cdot \begin{bmatrix} i_\alpha^s(t) \\ i_\beta^s(t) \\ i_d^r(t) \\ i_q^r(t) \end{bmatrix} + \tag{4}$$

$$+ \begin{bmatrix} R_1 & 0 & 0 & 0 \\ 0 & R_1 & 0 & 0 \\ 0 & \frac{3}{2}pM\Omega(t) & R_2' & p\Omega(t)\left(L_2'+\frac{1}{2}M\right) \\ -\frac{3}{2}pM\Omega(t) & 0 & -p\Omega(t)\left(L_2'+\frac{1}{2}M\right) & R_2' \end{bmatrix} \cdot \begin{bmatrix} i_\alpha^s(t) \\ i_\beta^s(t) \\ i_d^r(t) \\ i_q^r(t) \end{bmatrix},$$

where U denotes the power supply voltage, f_0 is the electric network frequency, L_1, L_2' are the stator coil inductance and the equivalent rotor coil inductance, respectively, M denotes the relative rotor-to-stator coil inductance, R_1, R_2' are the stator coil resistance and the equivalent rotor coil resistance, respectively, p is the number of pairs of the motor magnetic poles, $\Omega(t)$ is the current rotor angular velocity including the average and vibratory component and i_α^s, i_β^s are the electric currents in the stator reduced to the electric field equivalent axes α and β and i_d^r, i_q^r are the electric currents in the rotor reduced to the electric field equivalent axes d and q, [10]. Then, the electromagnetic torque generated by such a motor can expressed by the following formula:

$$T_{el} = \frac{3}{2}pM\left(i_\beta^s \cdot i_d^r - i_\alpha^s \cdot i_q^r\right). \tag{5}$$

2.3 Analysis of the electromechanical interaction

From the system of Park's equations (4) as well as from formula (5) it follows that the coupling between the electric and the mechanical system is non-linear in character, particularly for significantly varying motor rotational speed $\Omega(t)$, which leads to very complicated analytical description resulting in rather harmful computer implementation. Thus, this electromechanical coupling can be realized here by means of the step-by-step numerical extrapolation technique, which for relatively small direct integration steps for equations (2) or (3) results in very effective, stable and reliable results of computer simulation. Nevertheless, for steady-state operating conditions with the constant average motor rotational speed Ω_n, i.e. for $\Omega(t)=\Omega_n+\Theta(t)$, where $|\Theta(t)|<<\Omega_n$, in order to obtain more qualitative information about the character of electromechanical coupling in the drive system, the harmonic balance method has been applied in [5] for an approximate analytical solution for currents in Park's equations. Subsequently, for the assumed sinusoidal external excitation generated by the driven machine $M_r(t)=R\cdot\sin(\omega t)$, the fluctuating component of the motor rotational speed $\Omega(t)$ is expected also in the harmonic form: $\Theta(t)=G\cdot\sin(\omega t)+H\cdot\cos(\omega t)$, where $|G|,|H|<<\Omega_n$. Then, according to [5], for $\Omega(t)=\Omega_n+\Theta(t)$ an application of the harmonic balance method leads to the system of linear algebraic equations mutually combining dynamic properties of the electrical and mechanical parts of the considered object.

By solving that system of algebraic electromechanical equations and upon neglecting small terms of higher order, the fluctuating component of the motor torque is obtained in the following harmonic form:

$$T_{el}^{\mathrm{var}}(t) = S(\omega)\cdot\sin(\omega t) + T(\omega)\cdot\cos(\omega t). \tag{6}$$

For the abovementioned harmonic retarding torque generated by the driven machine working tool and for the obtained harmonic electromagnetic motor torque (6), the external excitations of modal equations (2) become also harmonic. By means of the well known analytical solutions of such ordinary differential equations and using the Fourier solution, dynamic responses of the considered mechanical system can be determined. For example, the sine- and cosine-amplitudes of the fluctuating component of the motor rotational speed $\Theta(t)$ are then obtained in the following form:

$$G = -\omega \cdot W,\ W = \sum_{m=0}^{\infty} \frac{(X_m^S)^2 T(\omega)\cdot(\omega_m^2 - \omega^2) - \left[(X_m^S)^2 S(\omega) - X_m^S X_m^R R\right]\cdot(\beta + \tau\omega_m^2)\omega}{\gamma_m^2\left[(\omega_m^2 - \omega^2)^2 + (\beta + \tau\omega_m^2)^2\omega^2\right]} \tag{7}$$

and $$H = \omega \cdot U,\ U = \sum_{m=0}^{\infty} \frac{\left[(X_m^S)^2 S(\omega) - X_m^S X_m^R R\right]\cdot(\omega_m^2 - \omega^2) + (X_m^S)^2 T(\omega)\cdot(\beta + \tau\omega_m^2)\omega}{\gamma_m^2\left[(\omega_m^2 - \omega^2)^2 + (\beta + \tau\omega_m^2)^2\omega^2\right]}.$$

Then, by expressing in the abovementioned system of algebraic electromechanical equations the amplitudes G and H of the fluctuating component of the motor rotor angular velocity $\Theta(t)$ by means of (7), the amplitudes $S(\omega)$ and $T(\omega)$ of the motor torque fluctuating component become functions of the drive system electromechanical dynamic properties. Then, by projecting the sine- and cosine-components of the electromagnetic torque in (6) and of the rotor rotation angle respectively on the complex plane real and imaginary axes and using the proper definitions given e.g. in [3], the electromagnetic torsional stiffness $k_e(\omega)$ and coefficient of damping $d_e(\omega)$ generated by the asynchronous motor are determined in the following form:

$$k_e(\omega) = -\frac{U\cdot S(\omega) + W\cdot T(\omega)}{U^2 + W^2}, \qquad d_e(\omega) = -\frac{1}{\omega}\cdot\frac{U\cdot T(\omega) - W\cdot S(\omega)}{U^2 + W^2}, \tag{8}$$

where the sine- and cosine- angular displacement amplitudes U and W have been already defined in (7). The above expressions (6)-(8) derived by means of the proposed in [5] analytical-computational approach enable us to determine dynamic characteristics of the coupled electromechanical system.

2.4 Modelling of the electromechanical system

According to the considerations performed above, in steady-state operating conditions dynamic interaction of the asynchronous motor with the drive system can be reduced to a visco-elastic clamping of the motor rotor with the immovable stator by means of the electromagnetic spring of stiffness $k_e(\omega)$ and damping coefficient $d_e(\omega)$ expressed by formulae (8). Then, the studied 'free-free' torsional train presented in Fig. 1 becomes rotationally clamped along the motor rotor, as shown in Fig. 3. Thus, for the drive system operating with a constant average

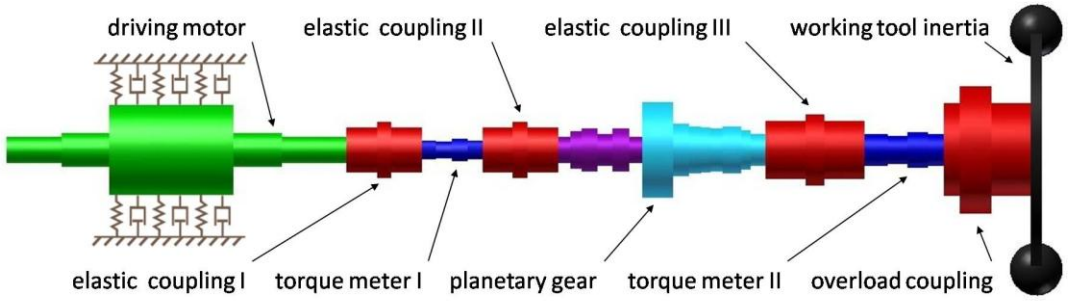

Figure 3: Hybrid electromechanical model of the drive system (regarded as a visco-elastically clamped)

rotational speed under steady-state harmonic excitation of frequency ω generated by retarding torques, the local motion equation for cross-sections of the k-th macro-element of length l_k representing the motor rotor is obtained now the following form:

$$G_k J_{\mathrm{E}k}\left(1 + \tau\frac{\partial}{\partial t}\right)\frac{\partial^2\theta_k(x,t)}{\partial x^2} - \frac{d_e(\omega)}{l_k}\frac{\partial\theta_k(x,t)}{\partial t} - \frac{k_e(\omega)}{l_k}\theta_k(x,t) - \rho\left(J_{\mathrm{E}k} + J_{\mathrm{I}k}\right)\frac{\partial^2\theta_k(x,t)}{\partial t^2} = 0. \tag{9}$$

Regarding the visco-elastic clamping terms in (9) as response dependent continuously distributed external excitations, the Fourier solution for forced vibrations can be also sought in the same as above base of orthogonal eigenfunctions. This approach leads to the analogous mutual coupling of modal equations (2), as in the case of equations (3) coupled by control torques generated by the linear magneto-rheological dampers. But here one obtains

$$\mathbf{M}_0\ddot{\mathbf{r}}(t) + \mathbf{D}(C_0(t,\dot{\mathbf{r}}(t)), d_e(\omega))\cdot\dot{\mathbf{r}}(t) + \mathbf{K}(k_e(\omega))\cdot\mathbf{r}(t) = \mathbf{F}(\omega t), \tag{10}$$

where: $\mathbf{D}(C_0(t,\dot{\mathbf{r}}(t)), d_e(\omega)) = \mathbf{D}_0 + \mathbf{D}_{\mathrm{C}}(C_0(t,\dot{\mathbf{r}}(t)) + \mathbf{D}_{\mathrm{E}}(d_e(\omega)),\quad \mathbf{K}(k_e(\omega)) = \mathbf{K}_0 + \mathbf{K}_{\mathrm{E}}(k_e(\omega)),$

the symbol $\mathbf{D}_E(d_e(\omega))$ denotes the full electromagnetic damping matrix, $\mathbf{K}_E(k_e(\omega))$ is the full electromagnetic stiffness matrix, $\mathbf{F}(\omega t)$ denotes the harmonic external excitation vector for the steady-state operating conditions of the considered drive system of a rotating machine and all the remaining symbols have been already defined in (3). It is to emphasize that for harmonic excitations with unitary amplitudes of $\mathbf{F}(\omega t)$, for selected constant control damping coefficients C_0 realized by the magneto-rheological dampers and assuming analytical harmonic solutions for vector $\mathbf{r}(t)$, by means of the system of modal equations (10) the frequency response functions for the considered object can be determined. In this way, qualitative analyses of the semi-actively controlled electromechanical system are going to be carried out in order to determine an influence of the electromagnetic motor torque on possible resonant- or dynamic amplification frequency zones of electromechanical interaction for various levels of control damping. Results of these investigations will be presented below in the computational example.

3 Computational example

The presented above analytical solution obtained for the electromechanical model will be applied for the coal pulverizer drive system driven by the asynchronous motor. Fundamental parameters of this four magnetic pole (p=2) motor are contained in Table 1. In the computational example the coal pulverizer is driven by the abovementioned motor by means of the reduction planetary gear of the resultant ratio 1:5.33.

Table 1: Fundamental parameters of the asynchronous motor

Nominal power [kW]	Nominal rotational speed [rpm]	Rated torque [Nm]	Supplied voltage [V]	Voltage supply frequency [Hz]
22	1465	143	400	50
Stator coil resistance R_1 [Ω]	Equivalent rotor coil resistance R_2' [Ω]	Stator coil inductance L_1 [H]	Equivalent rotor coil inductance L_2' [H]	Relative rotor-to-stator coil inductance M [H]
0.41	0.32	0.1250	0.1271	0.1217

In order to achieve the theoretical results of the electromechanical coupling analysis of the semi-actively controlled drive system possibly realistic, the assumed hybrid model has been experimentally validated and the optimum control damping coefficient realized by the magneto-rheological actuator was determined. For this purpose the mechanical model must have been tuned up to obtain a sufficiently good agreement between the calculated first torsional natural frequencies respectively with these determined by measurements using a proper hydraulic shaker exciting the real drive system with a harmonic signal in the range 0-150 Hz. Then, in nominal, steady-state operating conditions of the real object under the natural external excitation generated by the coal pulverizer, time-histories of the dynamic torques transmitted by the system input-, i.e. between the driving motor and the gear stage, and output-shaft, i.e. between the gear stage and the driven machine working tool, were registered using the torque-meters built in the mentioned shafts, see Fig. 2 and 3. The exemplary plots of these time-histories are presented by the grey lines in Fig. 4a. For the assumed theoretical variable external excitation generated by the coal pulverizer in the form of series of fundamental harmonic components of possibly the same

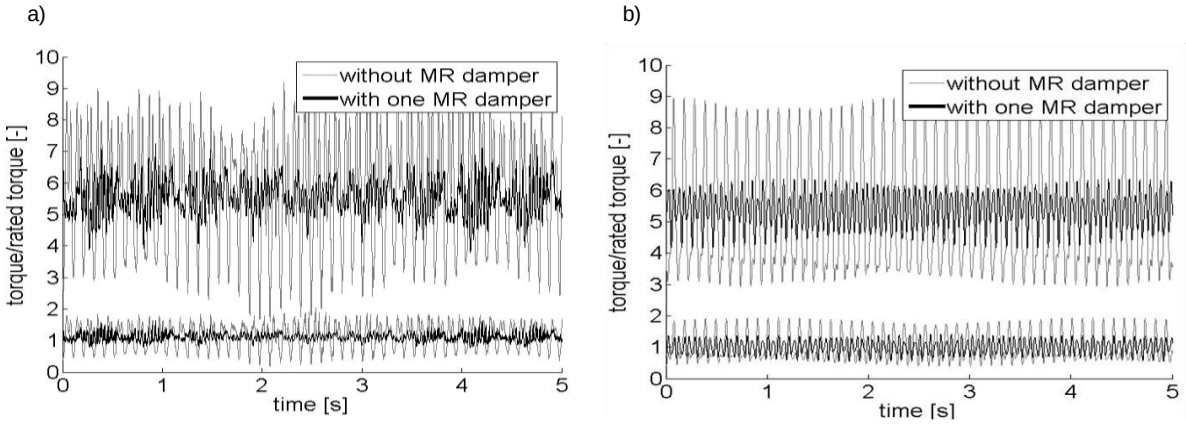

Figure 4: Time-histories of the dynamic torque transmitted by the input- and output-shaft obtained for the passive (grey) and semi-active (black) system by means of measurements (a) and simulation (b)

frequencies, amplitudes and phase angles respectively as these determined by means of the FFT analysis of the real signal, the analogous simulated time-histories have been obtained by means of solving the mutually independent modal equations (2) together with Park's equations (4) and relation (5) under the assumption of rigid suspension of the planetary gear housing and zero damping coefficient of the magneto-rheological actuator. The plots of these time-histories are depicted in Fig. 4b in the same way as the experimental ones in Fig. 4a.

For the aim of the electromechanical coupled qualitative analysis of the considered drive system for the given rotational flexibility of the gear housing suspension realized by the magneto-rheological dampers, the constant optimum value of the programmed control damping coefficient 135 Nms/rad has been determined experimentally and confirmed theoretically by means of numerical simulations based on coupled modal equations (3) together with relations (4) and (5). The obtained analogous results of dynamic torque time-histories are appropriately plotted in Fig. 4a and 4b by black lines. From the comparison of the mutually corresponding plots of time-histories registered for the input- and output-shaft it follows that for the determined optimum control damping coefficient ~60% reduction of torsional vibration amplitude values has been obtained experimentally and almost 65% reduction in the case of the theoretical results.

Then, by means of the experimentally tuned up drive system mechanical model together with the above determined optimum value of damping coefficient and using the contained in Table 1 parameters for the asynchronous motor circuit model the qualitative electromechanical interaction analysis can be carried out. The main considerations are going to be focused on the interaction frequency range ω containing the fundamental first system torsional eigen-frequencies in steady-state operating conditions under sinusoidal external excitation generated by the driven machine with the assumed test amplitude *R* equal to one half of the nominal torque which is quite common for crushers, mills, pulverizers, drilling devices and others. For this purpose, by means of formulae (6), (7) and the Fourier solution, in the retarding torque fluctuation frequency domain ω, in Fig. 5a the plots of steady-state dynamic response oscillation amplitudes are shown, where by the black and grey lines respectively the motor-torque and the input shaft dynamic torque amplitudes are plotted. It is worth noting that for the purely mechanical system first torsional eigenfrequencies equal to 4.2, 40.3 and 51.7 Hz, these almost entirely mutually overlying curves are characterized by the predominant amplitude peak of frequency ~2.1 Hz. This maximum dynamic response at ca. 2.1 Hz is of a quasi-static character being induced by very high electric motor torque amplitudes occurring at low interaction frequencies. The occurrence of these high amplitudes follows from the additional motor-torque characteristic determined for the arbitrarily assumed in frequency domain constant rotor angular velocity fluctuation amplitude and depicted by the dashed line in Fig. 5a.

In Fig. 5b, also in the retarding torque fluctuation frequency domain, there are presented by the black and grey lines, respectively, the plots of electromagnetic stiffness and damping coefficient determined using formulae (8). From the stiffness characteristic in Fig. 5b it follows that at the maximum dynamic response frequency 2.1 Hz the electromagnetic stiffness introduced by the asynchronous motor is equal ca. 0.180

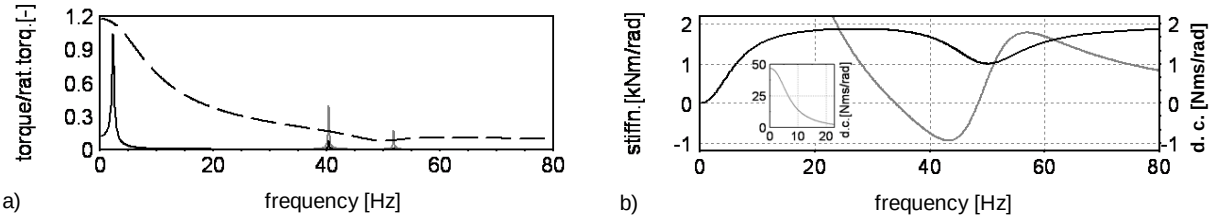

Figure 5: Amplitude characteristics of the electromagnetic torque (black) and mechanical torque in the shaft (grey) (a), electromagnetic stiffness (black) and damping coefficient (grey) (b)

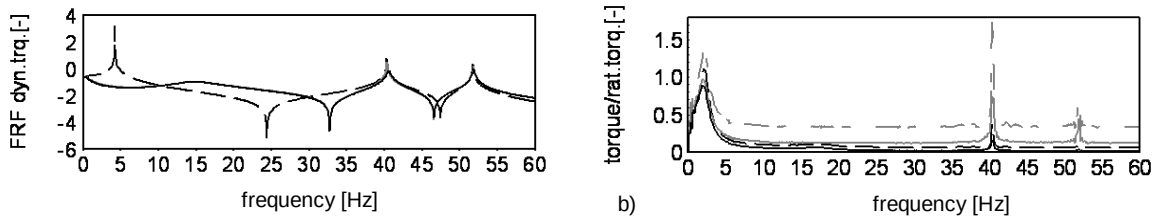

Figure 6: Frequency response functions of the mechanical passive (dashed), electromechanical passive (grey) and electromechanical controlled (black) system (a), amplitude characteristics of the electromagnetic torque (black) and dynamic torque in the shaft (grey) obtained for the passive (dashed) and controlled (solid) system (b)

kNm/rad, which for the motor location modal displacement equal to unity exceeds the mechanical system first modal torsional stiffness $\omega_1^2 \cdot \gamma_1^2$=0.169 kNm/rad, to reach much greater values for higher interaction frequencies. Thus, the considered drive system can not be regarded as a so called 'free-free' one, but it becomes visco-elastically clamped by the electromagnetic flux between the motor rotor and the stator. It is also worth noting

that the plot of the electromagnetic damping shown in Fig. 5b indicates a negative damping zone in the range between 35-50 Hz, which for very small drive system mechanical damping can lead to operational instabilities.

According to the above, by the use of such visco-elastically clamped model an influence of the asynchronous motor electromagnetic torque on drive system dynamic properties can be investigated. By means of the dashed line in Fig. 6a there is plotted the frequency response function of the purely mechanical passive drive system determined using Equations (10) for the harmonic excitation imposed on the driven machine working tool for $k_e(\omega)$, $d_e(\omega)$ equal to zero and for rigid rotational support of the planetary gear housing. The resonance peaks of this function confirm the abovementioned fundamental eigenfrequency values of the considered coal pulverizer drive system. By the grey line there is plotted the analogous frequency response function of the passive system visco-elastically clamped by means of the electromagnetic spring of the depicted in Fig. 5b interaction frequency dependent stiffness $k_e(\omega)$ and damping coefficient $d_e(\omega)$. From the comparison of these curves it follows that in the case of the frequency response function determined for the electromechanical system shown in Fig 3 the peak of frequency 4.2 Hz corresponding to the first natural frequency of the purely mechanical system has completely disappeared contrary to the further peaks related to the next two torsional natural frequencies equal to 40.3 and 51.7 Hz. In the considered case, such electromagnetic visco-elastic spring has completely attenuated the resonance effect with the first eigenfrequency because of relatively very high electromagnetic damping generated at low interaction frequencies, see Fig. 5b. The black line illustrates the frequency response function of the semi-actively controlled electromechanical system. This plot demonstrates, how the optimal control damping level realized by the magneto-rheological actuator suppresses possible resonances and non-resonant interaction frequency zones of torsional vibrations exited by the driven machine in steady-state operating conditions.

It is to emphasize that the presented above frequency response functions obtained for the clamped drive train model by means of the rotational visco-elastic spring of interaction frequency dependent stiffness and damping coefficient, on the one hand, quite clearly demonstrate the electromechanical system resonant and non-resonant dynamic properties, but on the other hand, not in an entirely complete way. Namely, the representation of the motor electromagnetic torque in the form of a visco-elastic spring, even in steady-state operating conditions, is rather passive in character and does not describe the asynchronous motor active sensitivity to generation of variable components of interaction frequency dependent amplitudes which follow from the electromechanical system dynamic torque characteristics shown in Fig. 5a. Apart of the resonant peaks corresponding to the second and the third system natural frequency, these characteristics contain the predominant abovementioned 'low-frequency' peaks of the quasi-static electromagnetic torque amplitude of frequency ca. 2.1 Hz, which almost overlays with the corresponding peak of the dynamic response torque amplitude.

According to the above, in order to demonstrate better this 'active' aspect of dynamic interaction of the asynchronous motor with the mechanical drive system as well as to examine an influence of semi-active vibration control using the magneto-rheological actuator, the numerical simulation approach has been employed basing on Equations (3) together with Park's equations (4) and expression (5). Here, successive simulations were performed for steady-state operating conditions in the most important range 0-60 Hz of the interaction frequency of harmonic excitation generated by the drive machine working tool with the frequency step value 0.1 Hz. In each case of interaction frequency ω, upon passages through transient operation states during system start-ups, maximal amplitudes of the motor electromagnetic torque fluctuation and of the dynamic torque transmitted by the system input shaft have been registered in the range of steady-state operating conditions, both for the passive system with the rigid gear housing support as well as for the optimally controlled system. The plots of the obtained in this way amplitude characteristics are depicted in Fig. 6b using the dashed black and grey lines corresponding respectively to the electromagnetic motor torque and the input shaft dynamic torque fluctuation amplitudes for the passive system and using the solid black and grey lines corresponding to the analogous torque amplitudes for the semi-actively controlled one. From this figure it follows that the amplitude characteristics determined for the passive system are qualitatively very similar to the analogous characteristics obtained by means of the analytical approach and presented in Fig. 5a. Subsequently, the amplitude characteristics determined for the controlled system, see Fig. 6b, confirm not only an ability of effective minimization of drive train resonant torsional vibrations similarly as the corresponding frequency response function plotted in Fig. 6a, but also an effective attenuation of the severe quasi-static oscillations induced by the motor electromagnetic torque due to the dynamic electromechanical interaction in the low frequency range in the vicinity of 2.1 Hz.

The results of qualitative analysis of an influence of the motor electromagnetic torque interaction on dynamic properties of the driven mechanical system carried out above can be illustrated by means of numerical simulation examples of selected dynamic responses in time domain. From results of numerical simulation performed for the resonant frequency 4.2 Hz of the retarding torque fluctuation it follows that completely no resonance effects are obtained, which indicate plots in Fig. 7a,b. In Fig. 7a by the black and grey lines there are respectively demonstrated time histories of the electromagnetic motor torque and of the driven machine retarding torque. In Fig. 7b there are depicted time histories of dynamic torques transmitted by the input (black line) and output (grey line) shaft during start-up and steady-state operation. The maximal amplification of the system dynamic response

has been obtained for the commented above retarding torque fluctuation frequency 2.1 Hz, which follows from the analogous results in Fig. 7c,d presented respectively in an identical way as these in Fig. 7a,b. In this way, there have been additionally confirmed the complete suppression of the resonance with the first mechanical system torsional eigenfrequency as well as the essential minimization of the quasi-static low-frequency excitation caused by the asynchronous motor electromagnetic torque.

Figure 7: Dynamic response of the coal-pulverizer drive system: for the resonant mechanical frequency (a,b) and for maximal vibration amplitudes (c,d)

Figure 8: Unstable dynamic response of the passive drive system (a,b) and the dynamic response stabilized by the semi-active control of the drive system (c,d)

The extremely small, but possible and still realistic, mechanical damping, i.e. below 1% critical, which is the very frequent case for many real torsionally vibrating shafts and drive systems, usually is not able to compensate the mentioned above negative electromagnetic damping, as in the interaction frequency range between 35-50 Hz shown in Fig. 5b. These situations can lead to operational instabilities, particularly if mechanical systems in such frequency ranges are characterized by a sensitivity to dynamic amplification. Actually, the considered system is characterized by a sensitivity to dynamic amplification in the form of possible resonance with the second drive system eigenform of frequency 40.3 Hz, as it follows from the frequency response function in Fig. 6a and the amplitude characteristics in Figs. 5a and 6b, all obtained for the assumed commonly applied material damping level equal to 3% critical for typical steel and cast iron parts of machine drive systems. But here, for the abovementioned very small mechanical damping, i.e. below 1% critical, the negative electromagnetic damping becomes predominant and leads to gradual rise of the electromechanical dynamic response amplitudes, as shown in Fig. 8a,b demonstrating in the same way as in Fig. 7 the simulation results obtained for the resonant interaction frequency 40.3 Hz. In order to avoid such quite probable dangerous scenarios of the drive system exploitation, the semi-active optimal control realized by the magneto-rheological actuator in the form of open-loop principle can be applied for the considered drive system. In Figs. 8c and 8d there are presented analogous as above results of numerical simulations obtained for the resonant excitation frequency 40.3 Hz for the controlled system. As it follows from the depicted dynamic torque time-histories, due to the external damping introduced into the system in the form of semi-active control, the torsional vibration amplitudes in the steady-state operation zone, i.e. for time greater than 1-1.5 s, remain on the stable, constant level.

4 Final remarks

In the paper dynamic electromechanical interaction between the semi-actively controlled drive system of a rotating machine and the driving asynchronous motor was studied. The theoretical and experimental research have been performed for the drive system of the coal pulverizer by the use of circuit model of the electric motor and by means of the structural hybrid mechanical model properly validated using measurements carried out on the real object. The theoretical study comprises a qualitative analysis of the electromechanical coupling effects by means of the approximate analytical solutions for the considered system mathematical model and using numerical simulations. From the obtained results of computations and measurements it follows that the asynchronous motor electromagnetic torque essentially changes dynamic properties of the mechanical system. First of all, the relatively high electromagnetic damping generated by the motor in the lowest frequency range of electromechanical interaction can completely suppress possible resonances with eigenforms of natural frequencies contained in this range. Moreover, low-frequency oscillation of the rotor angular velocity induces severe fluctuation of the driving motor torque resulting in drive system severe torsional vibrations of the quasi-static character, amplitudes of which can exceed amplitudes of possible ordinary resonances. The abovementioned electromagnetic damping is often characterized by negative values in given ranges of electromechanical interaction, what for the commonly observed low material damping in the torsionally vibrating drive systems and rotating machines can lead to dynamic instabilities or particularly severe resonances. It turned out that the proposed semi-active control of torsional vibrations by means of the actuators with the magneto-rheological fluid is able to attenuate effectively vibration amplitudes in resonant and non-resonant operating conditions as well as to minimize the abovementioned quasi-static oscillations induced by the low-frequency interaction of the drive system with the asynchronous motor. This fact has been also experimentally confirmed for numerous cases of steady-state operating conditions. Moreover, the additional external damping introduced into the mechanical system in the form of semi-active control effectively compensates the negative electromagnetic damping generated by the driving motor. In this paper the optimally selected open-loop control resulted in very efficient attenuation of torsional vibrations. Nevertheless, the closed loop approach of semi-active control is going to be tested in the electromechanical drive systems in the next steps of research.

Acknowledgement

All these investigations are supported by the Polish National Science Centre of the Ministry of Science and Higher Education: – Research Project No N 509 5376 40**.**

References

[1] Concordia, C. (1952): Induction motor damping and synchronizing torques. AIEE Transactions on Power Apparatus and Systems, Vol. 71, pp. 364-366.

[2] Del Puglia, S., De Franciscis, S., Van de Moortel, S., Jörg, P., Hattenbach, T., Sgrò, D., Antonelli, L. and Falomi, S. (2010): Torsional interaction optimization in a long train with a load commutated inverter. In *Proc. of the 8th IFToMM Int. Conference on Rotordynamics*, Seoul, Korea, Sept. 12-15, pp. 994-1001.

[3] Holopainen, T.P., Repo, A.-K. and Järvinen, J. (2010): Electromechanical interaction in torsional vibrations of drive train systems including an electrical machine, In *Proc. of the 8th IFToMM Int. Conference on Rotordynamics*, Seoul, Korea, September 12-15, pp. 986-993.

[4] Laschet, A. (1988): *Simulation von Antriebssystemen*. Springer-Verlag, Berlin, London, New-York, Paris, Tokyo.

[5] Szolc, T. and Pochanke A. (2012): Analytical-computational approach to dynamic investigation of the electromechanical coupling effects in the rotating systems driven by asynchronous motors. In *Proc. of the 10th IMechE Conf. on Vibrations in Rotating Machinery*, London, UK, Paper C1326/066, pp. 753-764.

[6] Szolc, T., Jankowski, Ł., Pochanke, A. and Michajłow, M. (2011): Vibration control of the coal pulvelizer geared drive system using linear actuators with the magneto-rheological fluid. In *Proc of the 9th Int. Conference on Vibrations in Rotating Machines SIRM 2011*, Darmstadt, Germany, Paper ID-46.

[7] Szolc, T. (2000): On the discrete-continuous modeling of rotor systems for the analysis of coupled lateral-torsional vibrations, *Int. Journal of Rotating Machinery*, 6(2), pp. 135–149.

[8] Tabesh, A. and Iravani, R., (2005): On the application of the complex torque coefficients method to the analysis of torsional dynamics. *IEEE Transactions on Energy Conversion*, Vol. 20, No. 2, pp. 268-275.

[9] Tanaka, K., Nemoto, H., Takahashi, N., Fukushima, Y., Akita, Y. and Tobise, M. (2010): Measurement and simulation of forced torsional vibration with inter-harmonic frequencies in variable speed drive motor driven compressor. In *Proc. of the 8th IFToMM Int. Conference on Rotordynamics*, Seoul, Korea, September 12-15, pp. 844-851.

[10] White, D. C. and Woodson, H. H. (1959):): *Electromechanical energy conversion*. Wiley, New York.